지진하중을 받는 RC 박스터널의 확률론적 취약도 평가기법

허정원[1] · 리 타이손[2] · 강충현[3] · 곽기석[4] · 박인준[5*]

[1]정회원, 전남대학교 해양토목공학과 교수
[2]비회원, 호주 뉴캐슬대학교 박사과정생
[3]비회원, 전남대학교 해양토목공학과 박사후연구원
[4]비회원, 한국건설기술연구원 지반연구소, 선임연구위원
[5]정회원, 한서대학교 공항융합학부 공항토목전공 교수

A probabilistic fragility evaluation method of a RC box tunnel subjected to earthquake loadings

Jungwon Huh[1] · Thai Son Le[2] · Choonghyun Kang[3] · Kiseok Kwak[4] · Inn-Joon Park[5*]

[1]Member, Professor, Dept. of Ocean Civil Engr., Chonnam National University
[2]Doctral Student, School of Engineering, The University of Newcastle, Australia
[3]Post-Doctoral Research Fellow, Dept. of Ocean Civil Engr., Chonnam National University
[4]Senior Research Fellow, Geotechnical Engr. Research Institute, KICT
[5]Member, Professor, Dept. of Civil Engr., Hanseo University

***Corresponding Author :** Inn-Joon Park, geotech@hanseo.ac.kr

Abstract

A probabilistic fragility assessment procedure is developed in this paper to predict risks of damage arising from seismic loading to the two-cell RC box tunnel. Especially, the paper focuses on establishing a simplified methodology to derive fragility curves which are an indispensable ingredient of seismic fragility assessment. In consideration of soil-structure interaction (SSI) effect, the ground response acceleration method for buried structure (GRAMBS) is used in the proposed approach to estimate the dynamic response behavior of the structures. In addition, the damage states of tunnels are identified by conducting the pushover analyses and Latin Hypercube sampling (LHS) technique is employed to consider the uncertainties associated with design variables. To illustrate the concepts described, a numerical analysis is conducted and fragility curves are developed for a large set of artificially generated ground motions satisfying a design spectrum. The seismic fragility curves are represented by two-parameter lognormal distribution function and its two parameters, namely the median and log-standard deviation, are estimated using the maximum likelihood estimates (MLE) method.

Keywords: Soil-structure interaction, Fragility curve, Maximum Likelihood, Latin Hypercube sampling, Pushover analysis

OPEN ACCESS

Journal of Korean Tunnelling and Underground Space Association
19(2)143-159(2017)
https://doi.org/10.9711/KTAJ.2017.19.2.143

eISSN: 2287-4747
pISSN: 2233-8292

Received February 13, 2017
Revised March 17, 2017
Accepted March 21, 2017

초 록

지진하중으로 초래되는 지하터널 구조물의 손상에 대한 위험도를 예측하기 위해 이 논문에서 확률론적 취약도 평가절차를 개발하였다. 특히 지진취약도 평가에 필수 요소인 취약도곡선의 유도를 위하여 단순화된 방법론을 정립하는 데 중점을 두었다. 지반-구조물상호작용(SSI) 효과를 고려한 구조물의 동적응답거동을 추정하기 위해서 지중구조물에 대한 지반응답가속도법(GRAMBS)을 제안기법에 적용하였다. 또한, 푸시오버 해석을 통해 터널의 손상상태를 정의하고 라틴하이퍼큐브 샘플링(LHS) 기법을 사용하여 설계변수와 관련된 불확실성을 고려하였다. 적용된 기법의 개념을 보다 상세하게 설명하기 위하여 설계스펙트럼을 만족하도록 생성된 다수의 인공지진운동에 대해 수치해석을 수행하고 취약도곡선을 개발하였다. 두 매개변수 대수정규분포 함수로 지진 취약도곡선을 표현하는데, 여기서 두 매개변수인 중앙값과 대수표준편차는 최우추정(MLE)법을 사용하여 산정하였다.

주요어: 지반-구조물상호작용, 취약도곡선, 최우추정법, 라틴하이퍼큐브 샘플링, 푸시오버 해석

1. Introduction

With the development of society and the growing urban population, large underground structures play an important role in modern urban system (Kim et al, 2000). However, many recorded data show that underground structures would be seriously damaged or even collapsed under strong earthquake. In addition, so far, the risk assessment of tunnels has been based on empirical fragility curves derived from existing damage records in preceding earthquake. Therefore, it is necessary to develop a comprehensive methodology for assessing earthquake risk of tunnel structures (Kim et al., 2008).

It is well known that soil-structure interaction (SSI) analysis is one of the major methods to predict dynamic behavior of structures (Choi et al, 2000). Nonetheless, the main deficiency of this method is that the analytical procedure becomes computationally costly and challenging due to the infinite nature of the ground system. Hence, the ground response acceleration method (GRAMBS), an effective quasi-static method that can deal with the interaction of soil and structure behavior, is employed in this research to replace the SSI approach (Katayama, 1990). It notably improves effectiveness by cutting down the analytical time with still ensuring accuracy. In addition, there is an absence of professional guideline to define damage states of tunnels. In this paper, the data on different damage states is obtained by using pushover analyses (so-called static nonlinear analysis), and the uncertainties of material properties which are joined by the Latin Hypercube sampling (LHS). An extensive set of artificial ground shakes/motions are produced performing various levels of seismic intensity and the fragility or fragility curves are finally established by using the maximum likelihood estimates (MLE).

2. Procedure of Fragility Curve Derivation

There are number of factors that influence the fragility curve development process such as input ground shake, structural damage data, structural simulation method, analysis method, performance limit states, consideration of uncertainties, etc. Therefore, to establish a frame work for the study, the derivation process used in this study is broken down into sub-tasks as shown in Fig. 1. The proposed methodology is proposed to create a new comprehensive numerical estimation scheme for the fragility evaluation, especially focusing on the integration of GRAMBS and MLE. However, it should be noted that the methodology contains two limitations discussed below. In particular, GRAMBS is not an extensive dynamic analysis method; it is a very effective and efficient quasi-static method that can deal with the soil-structure interaction behavior of underground structures subjected seismic loadings. In addition, the definitions of damage states used in this study might be conservative because they are based on the given numerical model together with consideration of both the performance levels in ATC-40 and the plastic hinges defined in FEMA 356.

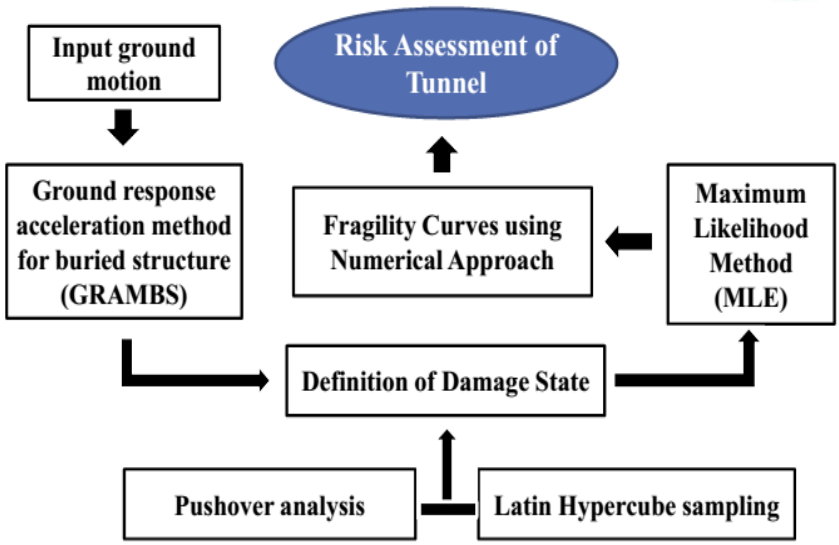

Fig. 1. Generic flow chart of the proposed methodology

2.1 Input ground motion

Due to the lack of sufficient and suitable earthquake records in Korea, a set of ground shakes are exploited for the derivation of fragility curves in this study in consideration of the design spectrum mentioned in KBC (KBC 2013). Eleven different seismic levels (IM's) are considered and 50 time histories of accelerations are

artificially generated per each IM by using QuakeGem program (Kim, 2007). Thus, 550 time histories are produced as the input data for the 1-D equivalent linear analysis of free-field ground. Finally, spectral matching is performed and response spectrums are derived for each IM to compare with the design target spectrum. The process is illustrated in Fig. 2.

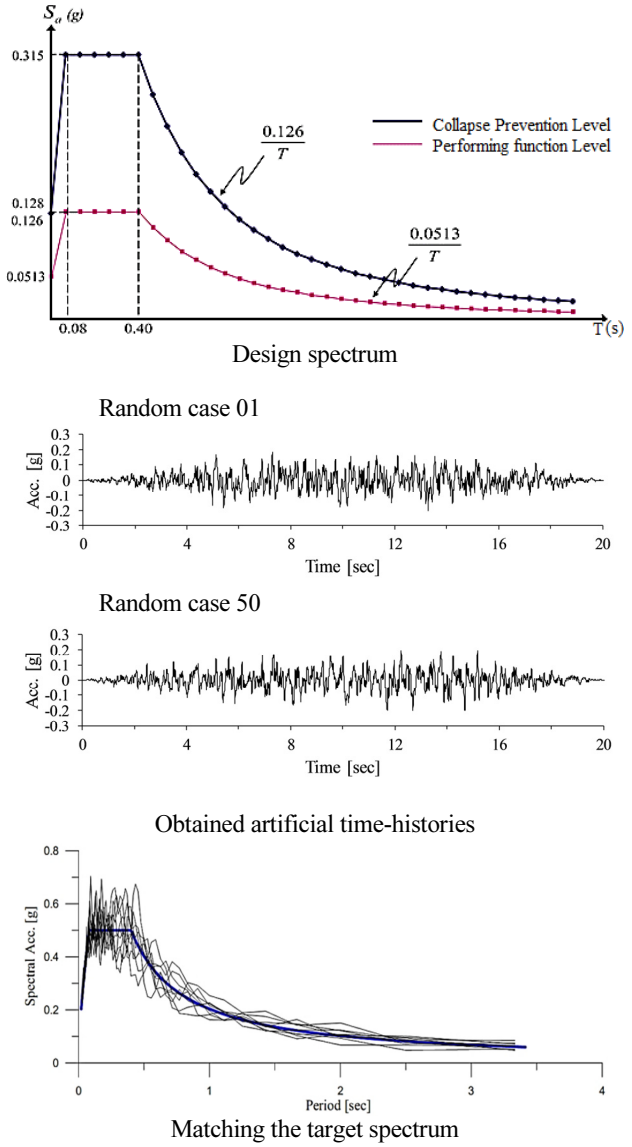

Fig. 2. Ground motion generation

2.2 Simplified response acceleration method for buried structures

In soil-structure system, the major external force to the structure is provided by the effective dynamic response of the surrounding soil. The dynamic problem of such buried structures certainly becomes the quasi-static interaction problem of the system consisting of a structure and its surrounding soil. When this two-dimensional system is excited by the horizontal input ground acceleration $\ddot{Z}(t)$, the equation of motion is provided below (1).

$$[M]\{\ddot{X}(t)\}+[C]\{\dot{X}(t)\}+[K]\{X(t)\}=-[M]\ddot{Z}(t) \tag{1}$$

Here [M], [C] and [K] are the mass, damping and stiffness matrix, respectively. X(t) represents the relative displacement vector.

At first, the actual tunnel is neglected and the system is assumed to consist only of the layer soil. The problem therefore turns out to be the free-field response of a uniform soil. The stress of a small portion of the soil from the depth j to j+1 can be expressed as (2).

$$S^j=[D][B]u^j \tag{2}$$

where Sj represents the stress of the soil from the depth j to j+1, [D] and [B] are the stress matrix, and uj is the relative displacement between the depth j and j+1

When Sj reaches maximum then uj must be maximum and (1) can be rewrite as (3).

$$[K]\{X(t_m)\}=-[M](\{\ddot{X}(t_m)\}+\ddot{Z}(t_m))-[C]\{\dot{X}(t_m)\} \tag{3}$$

Where the right hand side is the dynamic force applied on the whole system at time tm. Because the time is fixed, it becomes the solution of static problem

If the damping of the soil is small, (3) can be approximated as (4).

$$[K]\{X(t_m)\}=-[M](\{\ddot{X}(t_m)\}+\ddot{Z}(t_m)) \tag{4}$$

If the portion of the soil is replaced by the tunnel, then the corresponding parts of the matrices [M], [K], [D] and [B] relating to the calculation of the maximum stress described earlier are replaced by those of the tunnel, and uj becomes equivalent to the ultimate relative displacement between the tunnel's top and bottom positions. Finally, the ultimate stress state of the tunnel surrounded by the soil is approximately predicted. The analysis procedure for the proposed GRAMBS is illustrated in Fig. 3.

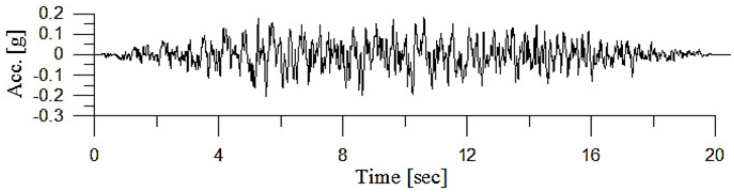

Artificial input time-history

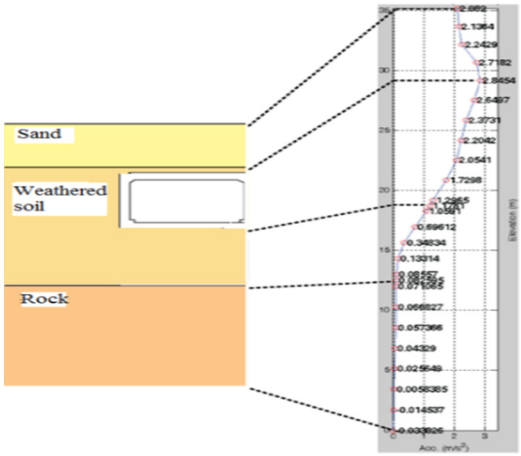

Free field response analysis result at tm

Fig. 3. GRAMBS process

In this study, the tunnel structure is ignored before analyzing the free-field ground response for each sub-layer. One-dimensional equivalent linear method is applied for this purpose based on M-SHAKE software (Kim, 2007). The main target is to estimate the responses of movement and acceleration at each sub-layer against time. Considering the time t_m (at the ultimate relative movement between the top and base slabs of the tunnel, the ground response acceleration at tm is taken all the full length of the ground depth and then converted it into the body forces. The corresponding displacement of the tunnel at time t_m can be obtained by conducting static analysis.

2.3 Damage state definition of two-cell RC box tunnels

Limit states values directly influence the fragility parameters. So, the definition of limit state is a key participant in the development of fragility curves. Although various damage indexes and corresponding parameters have been recommended for the fragility analysis of buildings and bridges, very limited information is available for tunnels. In this study, for damage indexes, the evaluation of damage is based on the deflection response of the structure. The damage states can be divided to three performance levels according to ATC40 (ATC40, 1996): Immediate Occupancy (IO), Life safety (LS), and Collapse Prevention (CP). They can be considered as minor (IO), moderate (LS) and extensive (CP) damage states, respectively. The pushover analysis, a simplified method to survey nonlinear behavior of the structure, is conducted for obtaining the maximum displacement capacity against each damage state.

The pushover analyses for the tunnel are carried out using nonlinear finite element analysis program (SAP2000) (www.eqrisk.info). The inelastic behavior of a beam can be modeled by using the concentrated or distributed hinge model. The concentrated hinge model is applied for cases where the yielding will most probably occur at the member ends. The distributed hinge model is applied for cases where the yielding may occur along the member. In this study, the tunnel is considered as a frame structure and the yielding points are assumed to be developed at the end of frames. The hinge positions and typical hinge properties are represented in Fig. 4 and Fig. 5, respectively. AB represents the linear elastic range from unloaded state A to its effective yield B, followed by an inelastic but linear response of ductile stiffness from B to C. C to D shows a sudden reduction in load resistance.

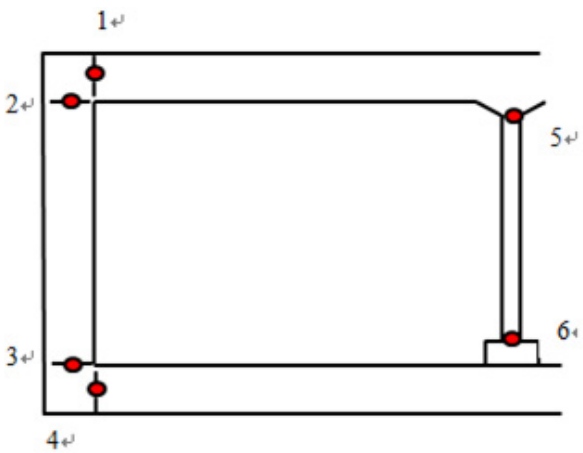

Fig. 4. Inspection point for the hinge model

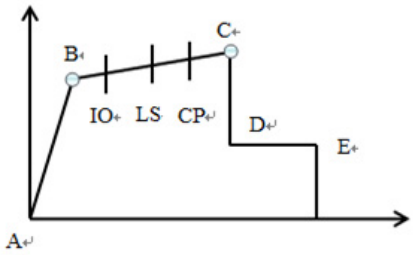

Fig. 5. Typical hinge properties and defined damage states

The gradual load increment is applied to generate displacement from initial state to the ultimate. The tunnel is assumed to be placed in one homogeneous ground deposit and two different pseudo-static lateral force models are applied to produce unit displacement at the highest position of the tunnel (Wang, 1993). These models are illustrated in Fig. 6.

(a) Simple model for deep tunnels: The shear force developed at the exterior surface of the roof is the primary cause of the structural racking. Thus, the racking effects of deep rectangular tunnel can be simulated by applying point/concentrated loading at the highest top of the wall.

(b) Distributed load model for shallow tunnels: Due to the decrease in soil cover, the cause of structural racking is shifted to the normal earth pressures developed along the side walls. Therefore, the racking deformation should be imposed by applying an inverted triangular displacement loading along the wall depth.

Simple pushover

Distributed pushover

Fig. 6. Pushover analysis model

The variability of material strength is often used as a major resource that controls the uncertainty of a reinforced concrete structure. Statistical variation of the material properties can be described by the mean and standard deviation. Thus, random variations and their statistical properties are both used for considering uncertainties, as shown in Table 1 (Matos et al., 2010) . There are several sampling methods can be used to generate random variables. Among the available sampling methods, the Monte Carlo simulation is a powerful tool and is the most widely used. However, there are disadvantages of using this method which is need a very large set of samples to meet the required accuracy. Therefore, in this paper, random variation is produced using the alternative approach, LHS method. This technique provides a stratified-random procedure in lieu of the natural random sampling that used in the Monte Carlo approach.

Twenty different pushover capacity curves for each model are described in detail as shown in Fig. 7. The relationship between displacement DM of the tunnel and seismic IM (herein peak ground acceleration) can be clearly acquired from the pushover approach as illustrated in Table 2. The damage index, denoted as DI, is

Table 1. Statistical property of the random variables

Random variables		Unit	Distribution	Mean	COV
Elastic modulus	Ec	GPa	Normal	30.00	0.150
Poisson's ratio	n		Normal	0.17	0.050
Compression strength	fc	MPa	Normal	28.00	0.100
Yield strength	σ_y	MPa	Normal	400.00	0.050
Concrete cover	t	mm	Normal	80.00	0.063

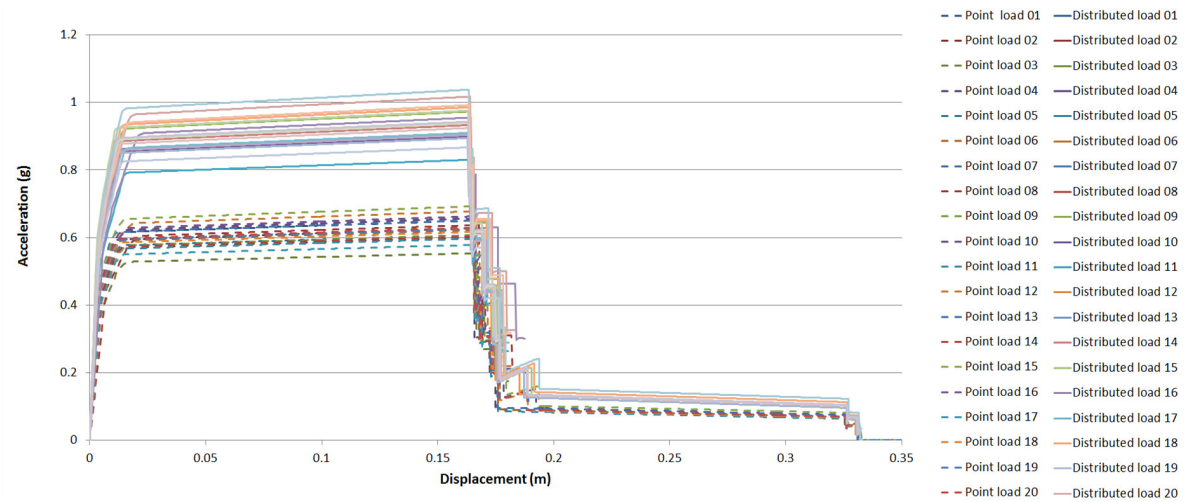

Fig. 7. Inspection point for the hinge model

Table 2. Values of damage state defined from pushover analysis

Case	Simple pushover						Distributed pushover					
	Minor damage		Moderate damage		Extensive damage		Minor damage		Moderate damage		Extensive damage	
	DM (m)	IM (g)	DM (m)	IM (g)	DM (m)	IM (g)	DM (m)	IM (g)	DM (m)	IM (g)	DM (m)	IM (g)
01	0.0695	0.6289	0.1348	0.6435	0.1657	0.6504	0.0670	0.6289	0.1323	0.9626	0.1637	0.9730
02	0.0689	0.5813	0.1346	0.5941	0.1655	0.6002	0.0669	0.5813	0.1321	0.8908	0.1635	0.9000
…	…	…	…	…	…	…	…	…	…	…	…	…
…	…	…	…	…	…	…	…	…	…	…	…	…
19	0.0687	0.6055	0.1345	0.6193	0.1654	0.6258	0.0667	0.9081	0.1325	0.9288	0.1634	0.9385
20	0.0685	0.6091	0.1343	0.6231	0.1652	0.6296	0.0670	0.9125	0.1323	0.9333	0.1632	0.9431
Average	0.0691		0.1346		0.1657		0.0670		0.1324		0.1635	
DI (%)	0.9		1.7		2.1		0.9		1.7		2.1	

Table 3. Statistical property of the random variables

None	Minor (IO)	Moderate (LS)	Extensive (CP)
DI ≤ 0.9%	0.9% < DI ≤ 1.7%	1.7% < DI ≤ 2.1%	DI > 2.1%

prescribed as the ratio of the horizontal displacement and the height of the tunnel, which can be derived by obtaining the average of drift capacity at each performance level. Four different damage states and their DIs are presented in Table 3.

2.4 Fragility curve development

Response data are obtained in terms of drift capacity. After evaluating the probability of exceedance based on limit states at each earthquake intensity level, the fragility curve can be developed by marking out on a graph of calculated results versus intensity level. The distribution function to represent the fragility curves is considered as follows (Shinozuka et al., 2000)

$$\mathrm{P}(\mathrm{IM}=\mathrm{x})=\Phi\left(\frac{\ln(\mathrm{x}/\theta)}{\beta}\right) \tag{5}$$

where P(IM= x) is the probability of failure; $\Phi(\ )$, θ and β are the normal cumulative distribution function, the median and standard deviation of ln IM, respectively.

It is common that the failure fragility function is estimated by repeatedly scaling a ground shake until it causes failure of the structure (Vamvatsikos and Cornell, 2004). This process produces a set of IM values affiliated with the onset of failure for each ground shake. Thus, the fragility parameters can be calculated by the Method of Moments (MOM) (Ibarra and Krawinkler, 2005):

$$\ln\hat{\theta} = \frac{1}{n}\sum_{i=1}^{n}\ln(IM_i) \tag{6}$$

$$\hat{\beta} = \sqrt{\frac{1}{n-1}\sum_{i=1}^{n}\left(\ln\left(IM_i/\hat{\theta}\right)\right)^2} \tag{7}$$

where n stands for the number of ground shakes, IM_i is the IM value affiliated with onset of failure for the i ground shake.

However, the above method is not possible because there is lack of data from past earthquake records. In this approach, selecting different ground shakes at each IM level is chosen in place of using incremental dynamic analysis. Therefore, we do not get an IM value affiliated with the onset of failure for each ground shake, we alternatively have a fraction of ground shake at each IM level that caused failure. Obtained data of this type is illustrated in Fig. 8.

To deal with this problem, two parameters of mentioned distribution function are independently estimated using the MLE method. The likelihood function can be represented by considering each IM level as a Bernoulli experiment (Fitting Fragility Function):

$$\text{Likelihood} = \prod_{j=1}^{m}\binom{n_j}{z_j}p_j^{z_j}\left(1-p_j^{z_j}\right)^{n_j-z_j} \tag{8}$$

where pj expresses the probability that a ground shake with IM = x_j will cause failure, z_j is the number of

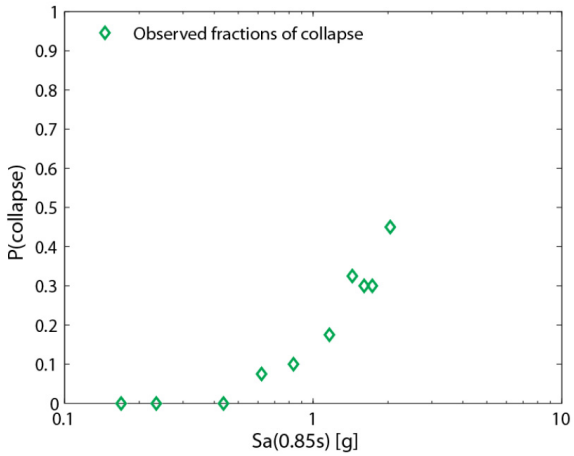

Fig. 8. Observed fraction of collapse

failure out of nj ground shakes, m describes the number of IM level.

The final target is to select a function that makes the highest probability of observing failure. Hence, fragility parameters can be gained by maximizing the likelihood function:

$$\{\hat{\mu},\hat{\theta}\} = \max \prod_{i=1}^{m} \binom{n_j}{z_j} \Phi\left(\frac{\ln(x_j/\theta)}{\beta}\right)^{z_j} \left(1-\Phi\left(\frac{\ln(x_j/\theta)}{\beta}\right)\right)^{n_j - z_j} \tag{9}$$

The parameters maximizing likelihood function (9) would also maximize the logarithmic likelihood function as shown below

$$\{\hat{\mu},\hat{\theta}\} = \max \sum_{i=1}^{m} \ln\binom{n_j}{z_j} + z_j \ln \Phi\left(\frac{\ln(x_j/\theta)}{\beta}\right) + (n_i - z_j)\ln\left(1-\Phi\left(\frac{\ln(x_j/\theta)}{\beta}\right)\right) \tag{10}$$

3. Numerical Simulation

The above concept is cleared up further with the support of a numerical simulation. A real one-story reinforced concrete tunnel with two cells shown in Fig. 9 is simulated. The tunnel height and width are 7.8 m and 29.3 m, respectively. The top and base slabs of the tunnel have their thickness of 1.2 m and 1.3 m, respectively. Deck slab is supported by two side walls with 1.0 m thick and a rectangular column in the middle with the dimension of 0.6 m × 0.7 m. The ground profile has three layers which are sand, weathered soil, and rock base. The soil and concrete properties in this study are summarized in Table 4 and Table 5 in details.

Table 4. Properties of reinforced concrete structure

Material	Poisson Ratio υ	Elastic Modulus Ec (KPa)	Unit mass ρ (t/m^3)	Damping
Concrete	0.17	28693	2.5	0.5

Table 5. Properties of soils

Soil name	Shear wave velocity (m/s)	Poisson Ratio	Unit weight (t/m^3)
Sand	275	0.35	1.8
Weathered soil	500	0.35	2.0
Rock	1500	0.35	2.3

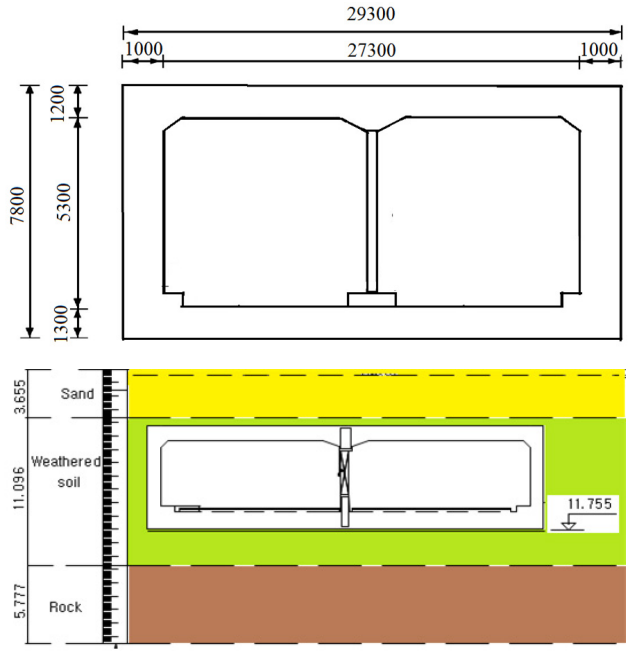

Fig. 9. Dimension and ground condition of the example

So far, finite element method (FEM) is known as the most powerful technique developed for numerical solution of complex problems in structural mechanics. In this study, a finite element mesh with traditional boundaries is adopted to model structure and soil conditions in Fig. 10. Both the soil and the concrete were modeled as linear elastic materials. The boundary side nodes are restrained vertically (only lateral displacements are possible), while the lower end node is restrained both vertically and laterally.

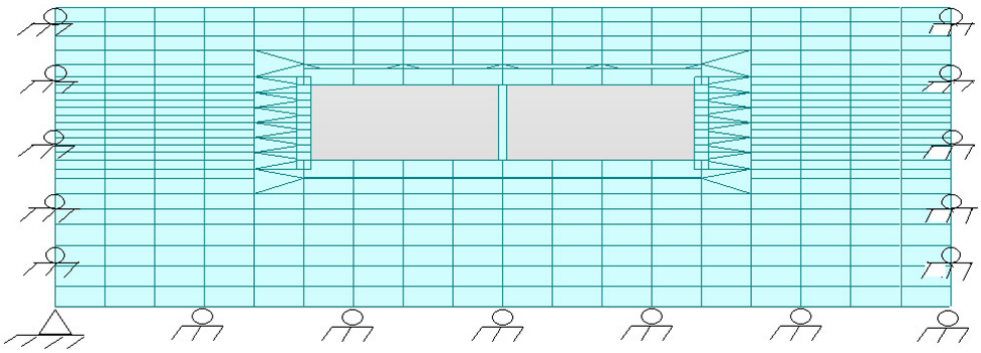

Fig. 10. Boundary model

Along all layers, body forces obtained from 1-D equivalent linear analysis by M-SHAKE [4], are applied to the tunnel structures in the static approach. The movements of the tunnel are picked up from static analysis using MIDAS Civil program (Midas Civil On-line Manual 2011). The probabilities of failure for three damage states with two pushover models, as presented in Table 2, are calculated for all eleven earthquake intensity levels in Table 6 where minor, moderate and extensive damage denote (1), (2), and (3), respectively and IM in this example is the peak ground acceleration.

Table 6. Probability of failure for different *IM*'s

IM (g)	Number of failure						Probability of failure					
	20 cases			50 cases			20 cases			50 cases		
	(1)	(2)	(3)	(1)	(2)	(3)	(1)	(2)	(3)	(1)	(2)	(3)
0.275	4	0	0	7	0	0	0.20	0.00	0.00	0.14	0.00	0.00
0.300	9	0	0	23	0	0	0.45	0.00	0.00	0.46	0.00	0.00
0.325	17	0	0	40	0	0	0.85	0.00	0.00	0.80	0.00	0.00
0.350	19	0	0	44	0	0	0.95	0.00	0.00	0.88	0.00	0.00
0.575	20	5	0	50	14	0	1.00	0.25	0.00	1.00	0.28	0.00
0.600	20	10	1	50	20	1	1.00	0.50	0.05	1.00	0.40	0.02
0.650	20	17	1	50	39	2	1.00	0.85	0.05	1.00	0.78	0.04
0.700	20	17	7	50	50	17	1.00	0.85	0.35	1.00	1.00	0.34
0.750	20	20	9	50	50	23	1.00	1.00	0.45	1.00	1.00	0.46
0.800	20	20	15	50	50	40	1.00	1.00	0.75	1.00	1.00	0.80
0.900	20	20	20	50	50	50	1.00	1.00	1.00	1.00	1.00	1.00

Two statistical parameters as mentioned in Eq. 10 are necessary to construct a fragility curve and the three fragility curves related to damage states are derived for both 20 and 50 cases. The median at each damage state is gained with its corresponding standard deviation summarized in Table 7.

Table 7. Summary of static parameter value

Damage state	20 cases			50 cases		
	Minor	Moderate	Extensive	Minor	Moderate	Extensive
Median θ	0.30	0.61	0.74	0.30	0.61	0.74
Standard deviation β	0.09	0.09	0.10	0.09	0.07	0.09

It can be recognized that fragility curves for the three damage states illustrated in Fig. 11 have identical shapes. The number of failures sharply rises with the trivial increase in the earthquake intensity level. The fragility curves gained from this research are found to be similar comparing those proposed by Pitilakis (Pitilakis, 2011). The reason might be due to the difference in the seismic analytical method and damage indexes. Carrying out more cases of pushover analyses can lead more stable results and accuracy of the damage indexes.

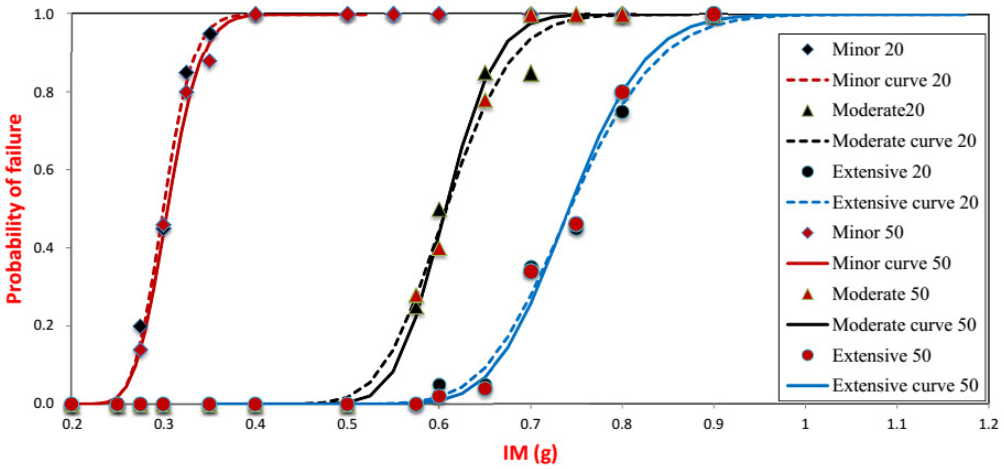

Fig. 11. Fragility curves for three damage states of the tunnel

In comparison, although the number of sampling increases from 20 cases to 50 cases, there is only a slightly decrease in the obtained β value from 0.09 to 0.07 and 0.10 to 0.09 in moderate damage and extensive damage, respectively. It states that the analysis with 20 ground shakes in each IM is a reasonable value for performing structural analysis to derive fragility curves of tunnels.

4. Conclusion and future work

By integrating GRAMBS and MLE, this study has proposed a comprehensive numerical estimation scheme for the fragility evaluation of the two-cell RC box tunnels subjected to earthquake loadings. It is involved with an illustrative example which proves computational effective. Furthermore, according to two-parameters data obtained from the example, the analysis with 20 ground shakes in each IM is considered as a rational value for performing structural analysis. As the same time, a professional guideline for damage states definition is also provided by carrying out pushover analysis and LHS to consider uncertainty of material properties.

The concept can be further extended in years to come by dealing with other uncertainties such as the

difference in geometric shapes of the two-cell RC ox tunnels or the variability of soil properties. There are rooms to improve the parameter estimation process for the seismic fragility function. Moreover, although the current research is for tunnel structures, the proposed methodology can be also applied to other underground systems such as pipelines and deep basement structure, etc.

Acknowledgment

This research was supported by Basic Science Research Program through the National Research foundation of Korea (NRF-2012R1A1A4A01015343 and NRF-2014R1A1A2058765) and the Korea Agency for Infrastructure Technology Advancement under the Ministry of Land, Infrastructure and Transport of the Korean government (Project Number: 13CCTI-T01).

References

1. Kim, J., Park, Y.J. You, J.S., Kim, D.H. (2000), “Development of Database System (GeoINFO) for the Investigation, Design and Construction of Underground Space”, Journal of Korean Tunnel and Underground Space Association, Vol. 10, pp. 506-515.
2. Kim Y.G., Kim, D.H. (2008), “Application of risk analysis and assessment considering tunnel stability and environmental effects in tunnel design”, Journal of Korean Tunnel and Underground Space Association, Vol. 10, pp. 1-15.
3. Choi, J.O., Kwon, O.S., Kim, M.M. (2000), “The Behavior of the Cast-in-place Pile Socketed in Rock Considering Soil-Structure Interaction”, Journal of Korean Tunnel and Underground Space Association, Vol. 10, pp. 457-468.
4. Katayama (1990), “Study on fundamental problems in seismic design analyses of critical structures and facilities”, Diss, Tokyo University, pp. 188-200.
5. KBC 2013, “Korea building code”.
6. Kim, J.M. (2007), “QuakeGem-Computer program for generating multiple earthquake motions”, Thesis, Chonnam National University.
7. Kim, J.M. (2007), M-Shake－Site response analysis for layered soil, Department of Civil and Environmental Engineering, Chonnam National University.
8. ATC40 (1996), “Seismic evaluation and retrofit of concrete building, California”.
9. Information on http://www.eqrisk.info/indo-nor-course/trainingsessions/Training_SAP2000NonLinear Analysis.pdf.
10. Wang, J.N. (1993), “Seismic design of tunnel: A state of the art approach”, Parsons Brinckerhoff monograph, Inc., New York.
11. Matos, J.C., Patista, J., Cruz, P., Valente, I. (2010), “Uncertainty evaluation of reinforced concrete

structures behavior", The fifth international Conference on bridge aintenance, safety and management-IABMAS 2010, International Association for Bridge Maintenance and Safety, Portugal.
12. Shinozuka, M., Feng, M.Q., Kim, H., Uzawa, T., Ueda, T. (2000), "Statistical analysis of fragility curves", Technical report MCEER.
13. Vamvatsikos, D., Cornell, C.A. (2004), "Applied incremental dynamic analysis", Earthquake spectra, Vol. 20, No. 2, pp. 523-553.
14. Ibarra, L.F., Krawinkler, H. (2005), "Global collapse of frame structures under seismic excitations", Berkeley, CA: Pacific Earthquake Engineering Research Center.
15. Information on http://web.stanford.edu/~bakerjw/fragility/archived_versions.
16. Information on http://manual.midasuser.com/EN_TW/civil/791/index.htm.
17. Pitilakis, K. (2011), "D3.7-Fragility function for Roadway System Elements", Norway.